GLUCOSE DETECTION WITH SURFACE PLASMON RESONANCE

SPECTROSCOPY AND MOLECULARLY IMPRINTED HYDROGEL

COATED SENSORS

by

Jing Wang

A thesis submitted to the Faculty of the University of Delaware in partial fulfillment of the requirements for the degree of Master of Science in Chemistry and Biochemistry

Summer 2011

GLUCOSE DETECTION WITH SURFACE PLASMON RESONANCE

SPECTROSCOPY AND MOLECULARLY IMPRINTED HYDROGEL

COATED SENSORS

by

Jing Wang

Approved: _____
Karl S. Booksh, Ph.D.
Professor in charge of thesis on behalf of the Advisory Committee

Approved: _____
Klaus H. Theopold, Ph.D.
Chair of the Department of Chemistry and Biochemistry

Approved: _____
George H. Watson, Ph.D.
Dean of the College of Arts and Sciences

Approved: _____
Charles G. Riordan, Ph.D.
Vice Provost for Graduate and Professional Education

ACKNOWLEDGEMENTS

And I am forever indebted to my parents, my love and friends for their endless encouragement and support.

This thesis is dedicated to my family.

TABLE OF CONTENTS

LIST OF TABLES

LIST OF FIGURES

ABSTRACT

Molecularly imprinted hydrogel membranes were developed and evaluated for detection of small analytes via surface plasmon resonance spectroscopy. Imprinting of glucose phosphate barium salt into a poly(allylamine hydrochloride) network covalently bound to gold surfaces yielded a selective sensor for glucose. Optimization of relative amounts of chemicals used for preparation of the hydrogel was performed to obtain highest sensitivity. Addition of gold nanoparticles into the hydrogel matrix significantly amplified its response and sensitivity due to the impact of gold nanoparticles on the refractive index of sensing layer. The detection limit of glucose in deionized water was calculated to be 0.02 mg/mL, well within the working concentration range suitable for glucose monitoring in diabetic individuals at physiological levels. Evaluation of its selectivity showed that the sensor displayed preferential recognition to glucose compared to structurally related sugars in addition to being unaffected by phosphate as well as compounds containing amine groups, such as creatinine. The developed sensor was finally exposed to human urine spiked with glucose illustrating its ability to selectively re-bind the analyte in complex matrices.

Chapter 1

INTRODUCTION

Detection and monitoring of small molecules, such as metabolites, drugs, pesticides, and pollutants has been of great interest in various field, including is of interest to environmental analysis, medical studies, clinical treatment and food science [1-7]. Often such measurements involve qualitative detection of analyte of low concentration and in complex matrices.

As a detecting technique, surface plasmon resonance (SPR) spectroscopy is a versatile approach capable of detecting a wide range of molecules upon incorporation of appropriate surface modification strategies , and is as well playing an important role in study on small molecule detection [8-13]. One most common configuration of SPR instrument, which was also employed in this research, is the Kretschmann configuration, in which surface plasmon polaritons (SPPs) are excited by backside-illuminating the plasmon supporting material (typically gold or silver) via total internal reflectance [14-16] as demonstrated in Figure 1.1.
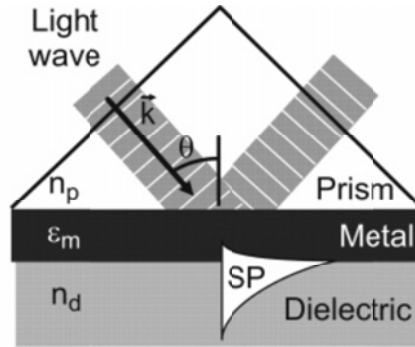
Figure 1.1 Demonstration of light coupling with surface plasmon (SP) on a metal surface. Figure is adopted from reference [15].

When a light wave was totally reflected at a metal surface, it generates an evanescent wave penetrating into the thin metal film, which at certain conditions can excite SPPs propagating along the surface. In SPR spectroscopic sensing measurements, the analytical signal is derived from the intensity minima of the reflected light (the so-called 'SPR dip'), which corresponds to the condition that allows the momentum component parallel to the metal surface of incident photons match that of excited SPPs, and is measured as a function of in-coupling angle (for monochromatic light sources) or wavelength (for fixed-angle configurations). The position of such minima responses to changes in the dielectric constant (ultimately, the refractive index, RI) of the sample induced by either chemical (e.g. antibody-antigen binding) or physical (e.g. temperature) events. SPR spectroscopy displays high sensitivity towards biomolecular binding events, as evidenced by low detection limits reported (ng/mL level [17,15]), as well as capability for real-time monitoring, rendering it an important tool in (bio)chemical analyses [15,18,19,16].

However, RI measurements are not inherently selective, therefore non-specific events originating from interferents present a challenge to SPR sensors. To overcome this limitation, different analyte recognition strategies have been incorporated [20].

Molecularly imprinted polymers (MIPs) and molecularly imprinted hydrogels (MIHs) have been developed for selective absorption of interested molecules. These materials consist of biomimetic matrices templated with a target analyte, yielding recognition sites shaped according the target inside the matrix, capable of selectively re-binding the analyte after removing template molecules [21]. These imprinted matrices have been regarded as an attractive approach towards improving sensor selectivity [22-25], due to their versatility, chemical robustness, simple preparation and long shelf-life compared to biosensing strategies (e.g., enzymes, antibodies). However, adoption of imprinted coatings for SPR sensing has thus far been limited despite initial positive reports from the literature [26,27,9,28].

Glucose detection is important for health monitoring in diabetic individuals [29,30]. Furthermore, accurate quantification of glucose in untreated physiological fluids, such as urine, remains challenging due to the complexity of the background matrix. Several examples of commercial glucose sensors are available; however, limitations on long-term storage compatibility, resulting from the use of enzymes for molecular recognition, has fueled investigations in alternative sensing strategies [31], with biomimetic materials, like MIPs, becoming a focus [32-34,24]. Hydrogels consist of a class of hydrophilic polymers capable of absorbing a high fraction of water [35,36], therefore diffusion, and ultimately detection, of polar glucose molecules through these hydrophilic membranes is facilitated. The coatings developed in this work consist of

cross-linked poly(allylamine hydrochloride) (PAH) templated with the D-glucose 6-phosphate monobarium salt (GPS-Ba), the hydrogel is then covalently bound to gold-coated glass slides to produce the chemical recognition sites. In addition to health monitoring, the use of glucose as the target analyte also provided a solid baseline with which to compare the performance of the strategy proposed to other sensing architectures available in the literature and in the market.

Binding site formation in molecular imprinting is largely driven by complexation of the template and monomers in solution *via* hydrogen bonding and π-π stacking [37-39]. Imprinting in solvents that disrupt hydrogen bonding interactions present an additional challenge which can be partially mitigated by employing a template baring a charge. Herein, self-assembly of the positively-charged polymer around the template is facilitated by the negatively charged phosphate group. Once the template is removed, detection of glucose (pure, not the barium salt) is achieved following RI changes resulting from physical swelling of the MIH upon binding of the analyte. This sensing platform can be prepared easily, used repeatedly and displays good sensitivity and selectivity towards concentrations lower than 5 mg/mL glucose in aqueous media. The structures of the template (GPS-Ba), analyte (glucose) and two structurally similar interferents involved in the study are displayed in Figure 1.2.

In contrast to detection of biomolecules, SPR sensing of small molecules remains largely unexplored due to the low RI changes induced by the analyte [14], ultimately translating into sensors with comparatively poor sensitivity requiring incorporation of a signal amplification method to improve limits of detection [40-42]. One approach used to improve sensor performance is by introducing gold nanoparticles into the chemical

recognition matrix [43,44]. In this case, the enhancement phenomenon can be attributed to either an increase in bulk RI due to the presence of nanoparticles and/or plasmonic coupling between the nanoparticles and the underlying continuous metal film [45-48,44,49,50]. Addition of nanoparticles to the MIH amplified the response of the sensor approximately 10-fold. The detection limit, sensitivity and selectivity of the sensor over sugars structurally similar to glucose suggests the ability to measure the analyte at physiologically relevant levels, as well as the prospect of applying similar detection strategies to other low molecular weight compounds.
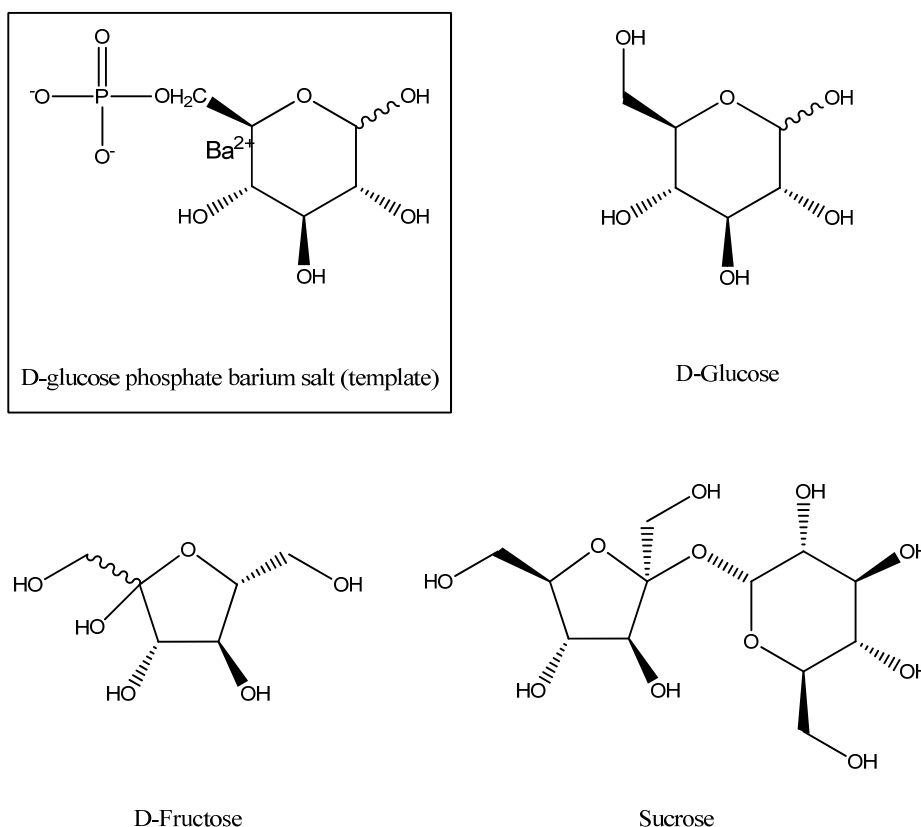
Figure 1.2. Structures of the template, the analyte (D-glucose) and two sugars structurally similar to glucose involved in the study.

Chapter 2

EXPERIMENTAL METHODS

2.1 Instrumental Configuration

Slides used for sensor preparation were made from either SF-10 (n=1.73) or BK-7 (n=1.52) glass and were coated with 5 nm chromium as an adhesion layer followed by 50 nm of gold by a Cressington 308R DC magnetron sputter coating system (Watford, UK). The SPR system was configured to use the Kretschmann arrangement where the sensor was back-side illuminated with a 5 watt Luxeon V white light LED (Lumileds Lighting, LLC, San Jose, CA) through a 60° equilateral prism of the same material as the slide, and the reflected light was transmitted via a linear array of optical fibers to a Jobin-Yvon SPEX 270M spectrometer (Horiba Jobin-Yvon, Edison New Jersey, NJ) with an 1200 g/mm grating. Spectra were collected with a 1024×1024 pixel TE-cooled CCD camera (Andor Technology, model DV435, South Windsor, CT). The spectrometer allowed light reflected from different positions on sensor surface being collected separately, therefore both the analytic and reference channels to be probed simultaneously on the same sensor. Each channel consisted of a strip 20 mm L $\times$ 4 mm W of the MIH coated sensor, though the spot size probed spectroscopically consisted of a 4 mm $\times$ 4 mm area in the center of each channel. The SPR shift measured corresponds to the response of the MIH coating to chemical stimuli over the 16 mm^2 area.

A demonstration of instrument setup is shown in Figure 2.1.
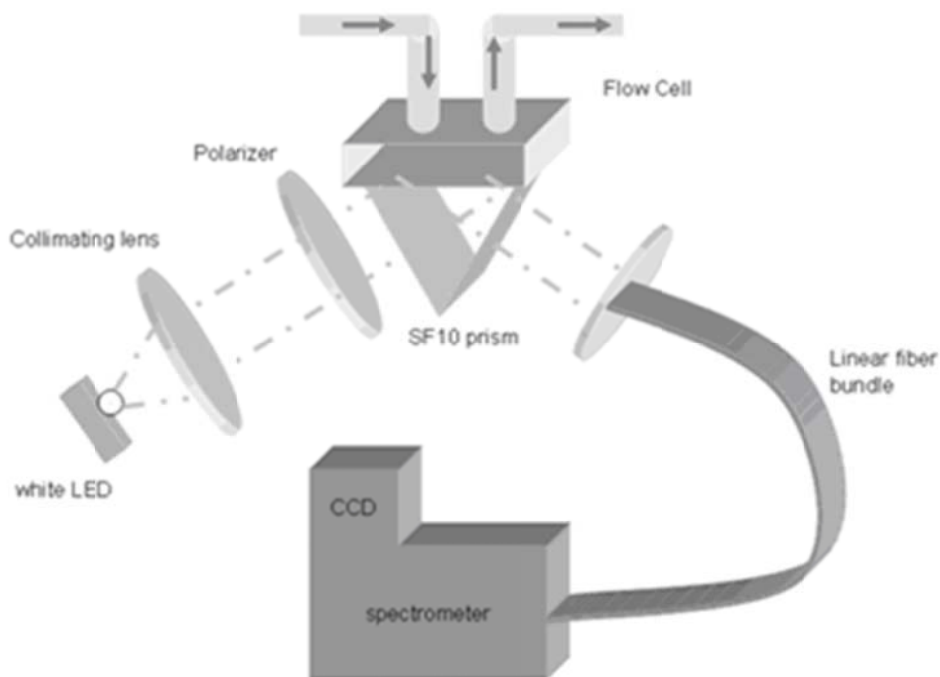
Figure 2.1. Demonstration of instrument setup.

2.2 MIH preparation

Two different self-assembled monolayers, formed from dithiobis(succinimidyl propionate) (DSP) and N-hydroxysuccinimide ester of 16-mercaptohexadecanoic acid (NHS-MHA) respectively, were evaluated for attachment of the MIH to sensor surfaces. DSP was purchased from Soltec Ventures, Inc. (Beverly, MA), whereas NHS-MHA was synthesized in-house following a previously described procedure [51].

DSP self-assembled monolayers were prepared by soaking freshly sputtered gold

surfaces in 0.001 M DSP in dimethylsulfoxide (DMSO, MP Biomedicals, Solon, OH). Similarly, for the NHS-MHA self-assembled monolayer preparation, sensor surfaces were exposed to 0.005 M NHS-MHA in tetrahydrofuran (THF, Fisher Scientific, Fair Lawn, NJ). Modified gold surfaces were rinsed with DMSO or THF (depending of the SAM used), and then with water before being immediately used in the MIH preparation process.

The MIH synthesis employed in this study was modified from Parmpi et al. [52] to yield membranes suitable for SPR analysis. Specifically, a 20 mL aqueous solution containing 0.1 mg/mL aqueous poly(allylamine hydrochloride) (PAH, Sigma–Aldrich, St. Louis, MO), 0.5 mg/mL D-glucose phosphate barium salt (GPS-Ba, Sigma–Aldrich, St. Louis, MO) and sufficient 1 M NaOH (Mallinckrodt, Paris, KY) to raise the solution pH to 9 (in order to partially neutralize the amine sites, rendering them available for subsequent tethering to the gold surface) was stirred for 30 minutes prior to addition of DSP-modified gold-coated slides. The 30 minute delay allows for interaction and re-arrangement of the PAH around the template, initiating the formation of the analyte-recognizing cavities [52,53]. After 3 hours, 5 mL of 0.03 M epichlorohydrin (Acros Organics, Morris Plains, NJ) were added to crosslink the hydrogel and the solution was stirred overnight. The slides were then removed from the solution, rinsed with deionized water and dipped in 4 M NaOH solution overnight to extract the template. Finally, sensors were dipped in stirred deionized water for 30 minutes to thoroughly rinse off the NaOH. Sensor slides with NHS-MHA were prepared similarly, except that 1 mg/mL GPS-Ba was added to the polymer solution and that 0.2 M NaOH was used to remove the template after imprinting. Finally the slides were dried under a stream of dry nitrogen

(Keen Compressed Gas, Wilmington, DE) and stored under atmospheric conditions until used. For FT-IR studies, sensor slides were sputtered with 5 nm chromium followed by 150 nm of gold and prepared as describe above. Mid-infrared absorption spectra were acquired with a Vertex 70 FT-IR spectrometer (Bruker Optics, Billerica, MA) equipped with a liquid nitrogen-cooled mercury-cadmium-telluride detector (Infrared Associates, Inc., Stuart, FL) at a 2 cm^{-1} resolution. Each spectrum represents an average of 100 scans. An AutoSeagull specular reflectance accessory (Harrick Scientific, Pleasantville, NY) permitted spectral collection at an incident angle of 87°. In order to minimize atmospheric contributions, the sample compartment of the FT-IR spectrometer was aggressively purged with dry nitrogen gas. Scanning electron micrographs were acquired using a XL-30 scanning electron microscope (FEI, Hillsboro, OR) equipped with a field emission electron gun and operating in environmental mode.

2.3 Gold nanoparticle preparation

Gold nanoparticles were synthesized by a modified Turkevitch method [54]. Initially, the pH of a 10 mL 0.001 M $HAuCl_4 \cdot 3H_2O$ (Acros Organics, Morris Plains, NJ) solution was adjusted to 7.2 with 1 M NaOH. The solution was heated to boiling and 5% (w/w) sodium citrate (Fisher Scientific, Fair Lawn, NJ) was added to achieve a 2:1 ratio between citrate and $AuCl_4^-$. The boiling solution was continuously stirred for 1 hour turning a wine-red color. The colloid solution was allowed to cool to room temperature at which point several drops of a 1 M cysteamine hydrochloride (Sigma–Aldrich, St. Louis, MO) in 1 M NaOH solution was added until the colloid solution turned blue, indicating

that the gold nanoparticles were modified with the cysteamine capping agent. A 5 mL aliquot of this solution was added to the PAH solution immediately prior to the addition of epichlorohydrin. When gold nanoparticles were used the volume of 0.03 M epichlorohydrin was also adjusted to 6.25 mL to maintain the concentration of cross-linker. Characterization of the synthesized nanoparticles was performed with a JEM-2000fx transmission electron microscope (JEOL, Tokyo, Japan) equipped with a lanthanum hexaboride electron gun using an acceleration voltage of 200 kV. An aliquot of the freshly synthesized colloid solution was drop-casted onto 200-mesh carbon-coated nickel grids purchased from SPI Supplies (West Chester, PA). Size distribution was determined with the DigitalMicrograph software from Gatan Inc. (Pleasanton, CA).

2.4 Sugar detection in aqueous media

For SPR measurements, a custom-made dual channel poly(methyl methacrylate) flow-cell was used to divide the sensor surface into two separate sensing regions and to guide flow of solutions across the sensor surface. One channel was presented with the analyte in solution, while the other served as a reference channel to account for signal drifting from pressure changes, temperature fluctuation or other external factors. The sensor was fixed to the flow cell with a gasket made from laboratory paraffin film (Parafilm, Pechiney Plastic Packaging, Menasha, WI). The liquid flowing system consisted of a Rainin Dynamax peristaltic pump model RP-1 (Rainin Instrument, LLC, Oakland, CA) and a series of valves connected by 1/16 inch polytetrafluoroethylene tubing and controlled by a custom-written LabView virtual instrument (National

Instruments, Austin, TX). Experimental runs began with the collection of s-polarized reflectance spectra used to normalize the light output from the source. Rotating the linear polarizer 90° the p-polarized component required for plasmonic coupling. The SPR dip minima was located using automated 'minimum-hunting' MATLAB (Mathworks, Natick, MA) routines.

Each sensing cycle began with equilibration of the coating in water, followed by exposure to the analyte and then a water washing step to remove non-specifically bound species. At the end of each cycle, 0.1 M NaOH was flushed to regenerate the sensor surface. Each step lasted 10 minutes. The MIHs were evaluated for rebinding affinity towards glucose and structurally related sugars, fructose and sucrose, at various concentrations. Glucose, fructose and sucrose were all obtained from Sigma–Aldrich (St. Louis, MO).

2.5 Glucose detection in human urine

Urine sample collected from a healthy (non-diabetic) human male was used to verify the performance of the sensor exposed to physiological fluids. Prior to analysis, the urine was centrifuged to remove any particulate matter and the supernatant was spiked with 0.5 – 5.0 mg/mL glucose. Ammonium phosphate (Fisher Scientific, Fair Lawn, NJ), urea, uric acid and creatinine (all from Sigma–Aldrich, St. Louis, MO) at physiologically relevant concentrations [55] were dissolved in deionized water and used to condition the sensor prior to the SPR measurements. The collection conditions were identical to measurements performed with deionized water.

Chapter 3

RESULTS AND DISCUSSION

3.1 MIH synthesis and characterization

Two SAMs with different carbon-chain lengths (C_3 vs. C_{16}) were tested for MIH attachment to the gold SPR surfaces with no discernible difference in coating quality. This is not surprising since in the application described herein, the SAM is utilized merely as an tether site for the MIH, therefore, the length of the carbon chain is inconsequential.

Two contrasting processes are responsible for the formation of MIH coatings: The first one involves the availability of primary amines in neutralized PAH for reaction via amide coupling with the succinimidyl end-groups of the immobilized SAM and subsequent cross-linking upon addition of epichlorohydrin. The second process relies on the remaining amine salts in PAH to associate with the negatively charged phosphate groups of the template, forming the analyte binding sites in the MIH. Hence, control of the ratio between protonated and unprotonated amine groups present in solution is necessary, since attachment and cross-linking of the hydrogel network as well as the imprinting process itself are affected.

Figure 3.1 summarizes the influence of the relative protonated and unprotonated amine concentration, as determined by pH, on attachment of the hydrogel to SAM-

modified gold surfaces and the imprinting of template into the hydrogel matrix as

evaluated by reflectance FT-IR spectroscopy.
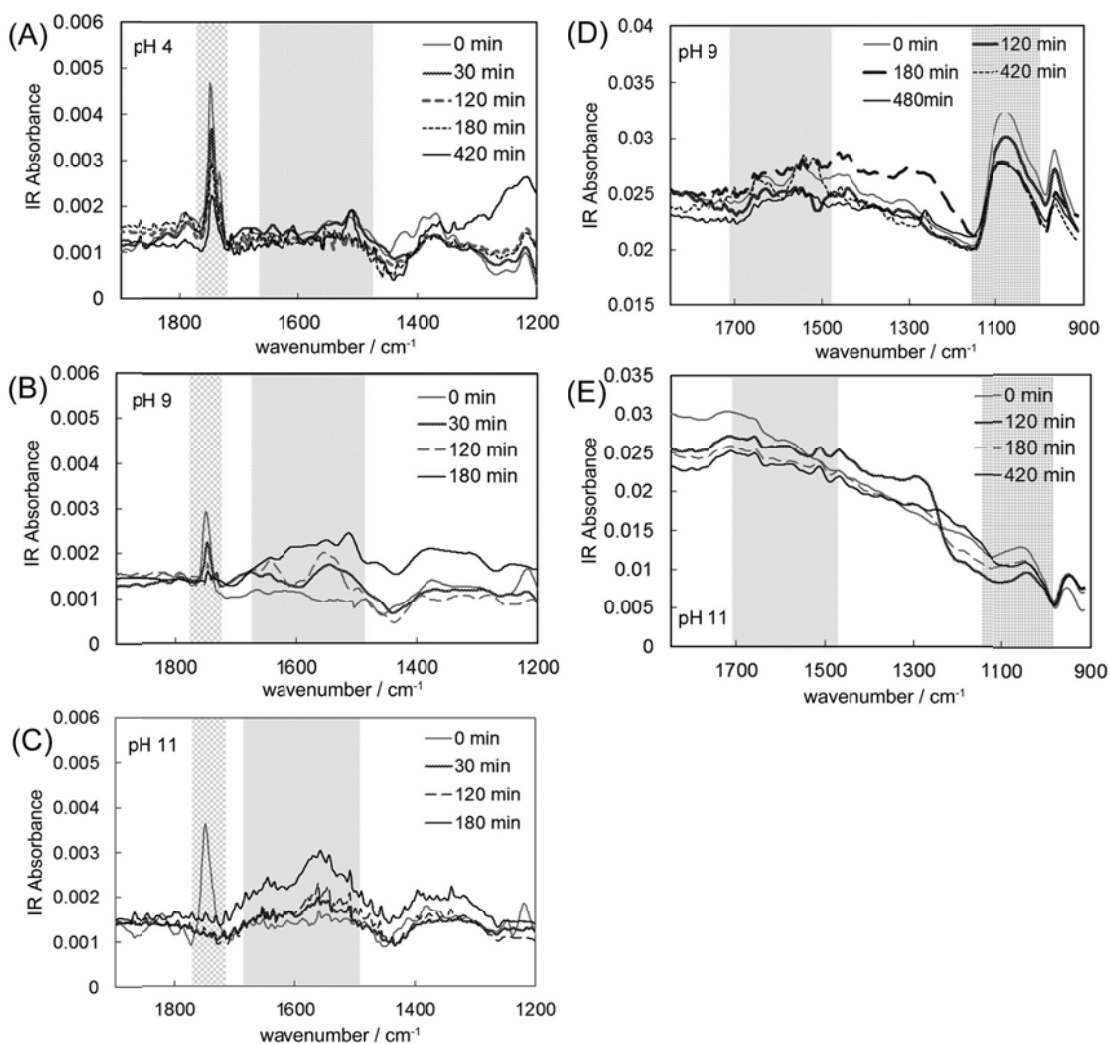
Figure 3.1. The attachment of polymer via NHS-MHA under (A) pH 4, (B) pH 9 and (C) pH 11, and the imprinting of GPS-Ba into PAH at (D) pH 9 and (E) pH 11 tracked by mid-IR spectroscopy. Each series of overlaid spectra corresponds to one slide. For (A), (B) and (C) spectra of slides coated with NHS-MHA were taken after the indicated time in 1 mg/mL polymer solution without template; for (D) and (E) spectra of slides imprinted and cross-linked were taken after the indicated time stirring in DI water. Absorption peaks of interest are highlighted by grey shadows.

PAH binding to SAM-modified surfaces can be monitored as a function of the decreasing $-C=O$ stretching peak absorbance at 1740 cm^{-1} associated with the NHS end-group. Concomitantly, the increasing symmetric and antisymmetric $-NH_2$ bands between 1500-1700 cm^{-1} further confirms attachment of the hydrogel to the surface [56]. At a pH value of 4 (see Figure 3.1(A)) the $-C=O$ peak was still prominent after a reaction time of 420 minutes, whereas it slowly decreases in intensity over 180 minutes at pH 9 (Figure 3.1(B)) and completely disappears within 30 minutes at pH 11 (Fig.1(C)). Comparison of the spectral time-series collected at the three pH values indicate that the rate of reaction between PAH and SAM concomitantly with the pH. The increase in intensity of the $-NH_2$ band confirms that amide coupling is favored at higher pHs. Estimation of the fraction of unprotonated amine groups in PAH (pKa ~ 9 [57,58]), yields that at pH values of 4, 9 and 11 the primary amines represent approximately 0.001%, 50% and 99%, respectively, of the total amines present in the hydrogel. Since unprotonated amines are responsible for reaction with the NHS leaving group and covalently bind to the SAM, the pH influences the binding rate of the hydrogel to sensor surfaces. Hydrogel attachment at pH 4 (Figure 3.1(A)) was not observed to occur to any appreciable extend, hence further studies focused exclusively on MIHs bound at pH values of 9 and 11.

Imprinting of the template was also evaluated by FT-IR spectroscopy. Using GPS-Ba as the template, instead of glucose, results in the formation of stronger GPS-Ba-hydrogel complex due to the ionic interaction. Because the MIH preparation is carried out in an aqueous environment, hydrogen bonding between glucose and amines cannot be relied on as the sole driving force for the imprinting process due to the interference of water [59,60]. Imprinting of the hydrogel with GPS-Ba yields an absorbance band at

approximately 1050 cm^{-1} associated with –P=O stretching of the phosphate group [56], indicating the incorporation of the template within the hydrogel. The FT-IR spectra in Figure 3.1(D) indicate that at pH 9, where approximately half of the amine groups are protonated, a strong association between the phosphate group and the PAH is achieved, as demonstrated by retention of the phosphate group within the hydrogel even after exposure to DI water for 6 hours. At pH 11 (Figure 3.1(E)), most of the amine groups are deprotonated, therefore the ionic interaction between the template and the hydrogel is not possible, resulting in a comparatively weak –P=O absorption peak. These results indicate that at pH 9 a good compromise is achieved between efficient hydrogel attachment to gold surfaces, while maintaining sufficient amine salts capable of interacting with the template. Hence, all hydrogel mixtures used for sensor studies presented below were adjusted to a pH 9.

In addition to PAH binding and extent of complex formation, the relative concentrations of the template, polymer and cross-linker require further tuning to yield a high SPR response. Different MIH synthesis parameters were evaluated with respect to the highest performance (i.e., $\Delta RI/\Delta C$[glucose]) by exposing the sensor to 10 mg/mL aqueous glucose solution. The results are summarized in Table 3.1.

Hydrogel coatings immobilized in the absence of GPS-Ba serve to establish a baseline 'control' response to non-selective diffusion of glucose through the hydrogel. Utilizing PAH concentrations below 1 mg/mL yielded non-reproducible batch-to-batch MIH membranes, therefore no data could be included in Table 3.1. In contrast, PAH concentrations approaching 2 mg/mL (coating 8) and higher produced broad SPR dips

(i.e. SPR coupling occurring at multiple conditions) due to coating heterogeneity within the plasmonically probed volume.

Table 3.1. Measure response to 10 mg/mL glucose in DI water for membranes prepared with different amounts of polymer, template and cross-linker.

Coating	PAH (mg/mL)	Epichlorohydrin (mg/mL)	GPS-Ba (mg/mL)	$\Delta\lambda_{SPR}$ (nm, $\mu \pm 1\sigma$)
1	1.0	0.2	0.0	0.15 ± 0.03
2	1.0	0.2	0.05	0.18 ± 0.05
3	1.0	0.2	0.5	0.28 ± 0.03
4	1.0	0.5	0.0	0.12 ± 0.04
5	1.0	0.5	0.05	0.14 ± 0.03
6	1.0	0.5	0.5	0.38 ± 0.05
7	1.0	1.0	0.5	0.35 ± 0.07
8	2.0	0.5	0.5	0.27 ± 0.05

Since measuring the response to the analyte is contingent upon precisely locating (in terms of wavelength) the SPR dip minima, broader dips render this procedure challenging. Coatings labeled 1 and 4 both serve as non-imprinted hydrogel (NIH) controls illustrating that non-selective absorption from a 10 mg/mL glucose solution yields a λ_{SPR} shift of approximately 0.15 nm. Addition of 0.05 mg/mL GPS-Ba (coatings 2 and 5) did not improve the response to the analyte beyond levels already attributed to non-specific interactions. Raising the concentration of the template to 0.5 mg/mL (coatings 3 and 6) resulted in the formation of sufficient template binding cavities to yield a statistically relevant λ_{SPR} shift. Comparison of MIHs formed with increasing levels of cross-linker (coatings 3, 6 and 7) indicate that structural rigidity of the hydrogel will influence the performance measured. From three epichlorohydrin concentrations

investigated, it is evident that "softer" hydrogels obtained at lower concentrations do not exhibit the same level of response to 10 mg/mL glucose as the two 'more rigid' counterparts. In part this may be due to the fact that a malleable carbon network is better capable of accommodating enriched analyte molecules within the free volume of the hydrogel, resulting in a lower degree of swelling. In contrast, a more rigid structure is forced to expand upon incorporation of the analyte since the carbon network in unable to re-adjust itself around the analyte.

Cross-linker concentration greater than 1 mg/mL were not pursued in this initial contribution because a structurally rigid coating, less amenable to swelling, and therefore displaying smaller λ_{SPR} shifts, is anticipated. For the binding studies presented herein, a cross-linker concentration of 0.5 mg/mL was used since it provided sufficient structural rigidity for selective cavities to retain their shape after template removal as well as enabling swelling of the MIH upon glucose re-binding.

3.2 Physical characterization

As was previously mentioned, RI changes monitored by SPR spectroscopy are non-selective. Therefore, discrimination of λ_{SPR} shift induced by bulk RI changes associated with solutions containing different glucose concentrations (e.g. a false positive) from λ_{SPR} shifts resulting from selective analyte uptake, is achieved by employing MIH membranes with thicknesses greater than penetration depth (d_p) of surface plasmons (approximately 200-300 nm [14]).

Scanning electron micrographs acquired along fractured edges provide an

approach for evaluating MIH thickness. By this method, MIH thickness ranged from approximately 0.8 μm to 2.5 μm. Therefore, λ_{SPR} shifts recorded reflect refractive index changes within the MIH rather than in the bulk liquid. The micrograph also reveals superficial accumulations ranging from 1 μm to 5 μm in size atop the relatively uniform background. The origin of these features is still unknown though it is likely that they correspond to hydrogel agglomerations formed in solution and bound to the coated sensor during later stages of MIH synthesis.

3.3 Glucose detection

Evaluation of MIH-coated sensors involved measuring glucose solutions with different concentrations. Sensor slides coated with MIH but without gold nanoparticles reached equilibrium response to the analyte within 2 minutes and displayed an increasing λ_{SPR} shift with glucose concentrations below ~5 mg/mL (Figure 3.2 (A)).
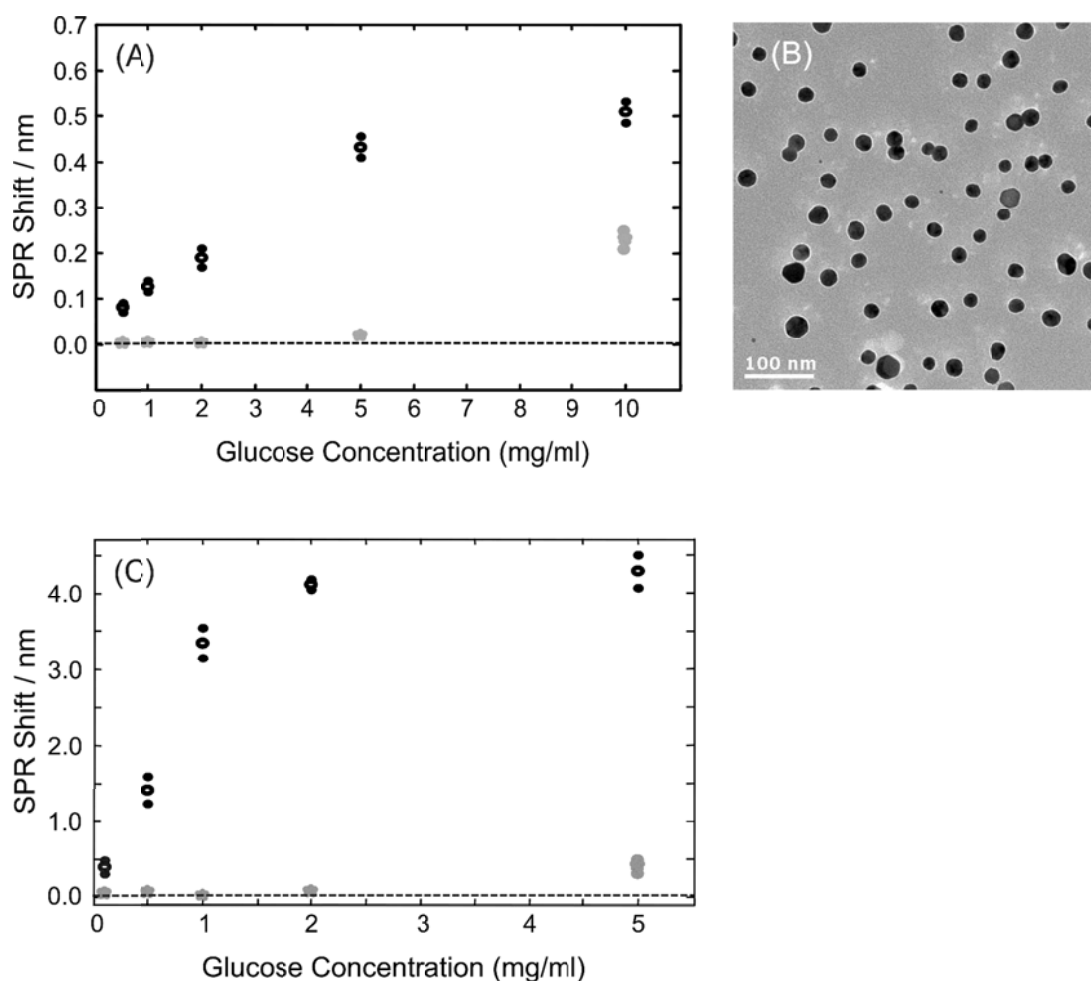
Fig 3.2. Sensor performance in aqueous glucose solutions and effect of gold nanoparticles. (A) SPR response of imprinted (black circles) and non-imprinted (grey stars) hydrogel sensor to glucose in DI water. Results came from different slides and error bars stand for 95% confidence interval. Precision of SPR shift is shown by plus/minus standard deviation of the mean (black dots, usually n=3). (B) A TEM image of gold nanoparticles used. (C) SPR response of imprinted (black circles) and non-imprinted (grey stars) hydrogel sensor embedded with gold nanoparticles to glucose in DI water. Results came from different slides and error bars stand for 95% confidence interval. Precision of SPR shift is shown by plus/minus standard deviation of the mean (black dots, usually n=3).

As was previously mentioned, control NIHs were prepared in exactly the same way as MIHs but without the template. In all measurements, the response obtained with

NIH was lower compared to imprinted hydrogels. Furthermore, NIH sensors required glucose concentrations greater than 5 mg/mL in order to register measurable shifts in λ_{SPR}. The difference in response between MIH and NIH suggest the presence of selective binding sites in the imprinted hydrogel, as well as indicating that non-specific interactions, such as surficial adsorption and non-specific diffusion of glucose, do not contribute significantly to the SPR response measured.

3.4 Addition of gold nanoparticles

The interaction between metallic nanoparticles, especially gold nanoparticles, and freely-propagating plasmons excited at continuous metal films has been previously described as a method for enhancing the SPR sensitivity [45,46,49,50,61,44,48]. In order to evaluate the influence of nanoparticles on MIHs, cysteamine-capped gold nanoparticles were embedded into the hydrogel by cross-linking the amine groups of the capping agent with unprotonated primary amines in PAH. An exemplary transmission electron microscopic image of the nanoparticles synthesized is shown in Figure 3.2(B). A distribution study of the images recorded indicates that the gold nanoparticles have a diameter of 25 ± 8 nm.

The response of MIH-coated sensors containing gold nanoparticles to aqueous glucose solutions of different concentrations is summarized graphically in Figure 3.2(C). Comparison with the results shown in Figure 3.2(A) demonstrate that addition of gold nanoparticles produces a 10- to 15-fold improvement in the amplitude of the SPR signal as well as increased sensitivity at low glucose concentrations (<1 mg/mL). In contrast,

control experiments with NIH membranes containing gold nanoparticles showed a comparatively small response to non-specific binding of glucose. The linear range of gold nanoparticles-MIH sensors decreased compared to MIH sensors without nanoparticles, as well as reaching saturation levels at lower glucose concentrations: 5 mg/mL versus 10 mg/mL for coatings with and without gold nanoparticles, respectively. A possible explanation for these observations is that the number of binding sites available inside the sensing layer is altered considerably by the incorporation of the nanoparticles. It may also be more difficult for glucose molecules to diffuse into the sensing layer during measurement when the layer is embedded with nanoparticles. Indeed comparison of the response of MIH and Au-MIH membranes to glucose shows that the presence of gold nanoparticles delays the onset of a stable response, as depicted in the sensorgrams shown in Figure 3.3.

The working concentration range of gold nanoparticles-MIH membranes cover the critical glucose concentrations in plasma tests [62,63] and urine glucose screening [64,65] for diagnosis of diabetes, and its upper limit is comparable to typical non-enzymatic glucose sensors reported [66-70]. From calibration, the limit of detection of the gold nanoparticle-MIH sensor in water was determined to be 0.02 mg/mL (S/N=3 based on standard deviation of the MIH response in a blank solution) and a limit of quantification of 0.06 mg/mL (based on 10 standard deviations of the MIH response in a blank solution) and a sensitivity of 1.9 nm/(mg/mL glucose) in deionized water.
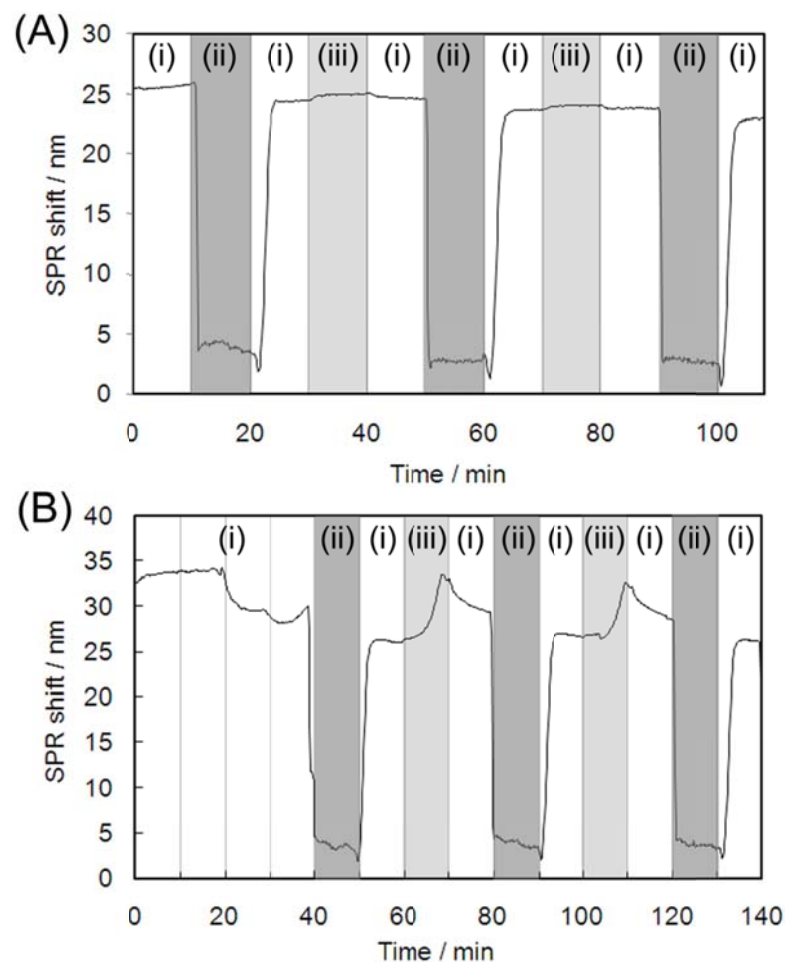
Figure 3.3. Exemplary sensorgrams of (A) MIH and (B) Au-MIH coated sensor detecting 1 mg/mL glucose in water. The sensor was rinsed with (i) deionized water, (ii) 0.1M NaOH and (iii) 1 mg/mL glucose.

Upon glucose binding and MIH swelling, a red-shift in the resonant wavelength was observed, which is in sharp contrast to the blue-shift expected from the increased distance between the gold nanoparticles and the underlying gold film (so-called "gap-mode" [47,48,71]). SPR responses are enhanced by plasmonic coupling if the distance, d, between the two plasmon active entities is maintained within the radius of the nanoparticle or smaller [72]. For the nanoparticles utilized herein, r ~13 nm. Considering

22

that the MIH synthesis was carried out by mixing all components in one vessel, it is likely that the nanoparticles are randomly distributed within the 0.8 μm thick membrane, and that most of them reside at d >13 nm. Therefore, the 10-fold increase in measured signal most likely rises from the increased bulk RI of the composite gold nanoparticles-MIH membrane.

It is worth noting that the comparatively large errors bars reported in Figure 3.2(C) result from measurements taken with different sensors, providing an estimate of batch-to-batch variability as opposed to variability within the same sensor. Glucose response was observed to decrease during repeated cycles, though this is possibly associated with the coating regeneration step which involves 0.1 M NaOH, used in order to ensure that all glucose is removed from the hydrogel but may also degrade the hydrogel.

3.5 Interference studies and glucose detection in urine

The formation of recognition sites for glucose in the sensing hydrogel is facilitated by ionic bonding of protonated amines in PAH with phosphate groups in GPS-Ba. Since a significant amount of phosphate (0.03-0.06 M) is present in urine [55] it is necessary to evaluate whether the presence of phosphate groups can interfere with the MIH ability to bind to glucose. Initial studies involving MIH coatings exposed to intermittent phosphate plumes did not show a net λ_{SPR} shift (i.e., the signal returned to baseline levels immediately upon flushing with deionized water) indicating that phosphate groups do not permanently re-bind to available amines in PAH (Figure

3.4(A)). Further investigation involving phosphate interferences revolved around using 0.06 M ammonium phosphate (titrated to pH 7) spiked with the analyte. Exemplary sensorgrams are depicted in Figure 3.4(B), which show a net λ_{SPR} shift due to glucose re-binding. The magnitude of the SPR response to glucose in phosphate solutions was similar to that obtained in DI water, suggesting that physiologically relevant levels of phosphate in urine are unlikely to interfere with glucose detection in complex matrices.

Finally, selective glucose recognition was examined by exposing the gold nanoparticles-MIH coatings to structurally similar. Figure 3.4(C) summarizes the λ_{SPR} shift measured with fructose and sucrose solutions. Fructose is structurally related to glucose, yet induces a significantly smaller response suggesting that although fructose is capable of binding to some of the recognition sites, the MIH preferentially binds to the template. The response measured with sucrose is even smaller than that for fructose. Sucrose is larger than either glucose or fructose, therefore, it is anticipated that the response will be affected by hindered diffusion through the MIH as well as size incompatibility with most of the recognition sites.

Cross-reactivity between molecularly imprinted materials and compounds structurally related to the template is common and can be minimized by careful choice of synthetic parameters (e.g. solvent, monomers) [73,74]; with regards to glucose monitoring, fructose has been previously recognized as a potential interferent [52,75,32]. This presents a challenge for sensing platforms aimed at single-compound detection in complex media. It has been suggested that an approach to mitigate cross-reactivity with molecularly imprinted materials involves the use of sensor arrays, wherein coatings with different specificities (analyte and interferents) are utilized and the response obtained is

24

mathematically treated to deconvolute the analytic from the interfering signal [76].
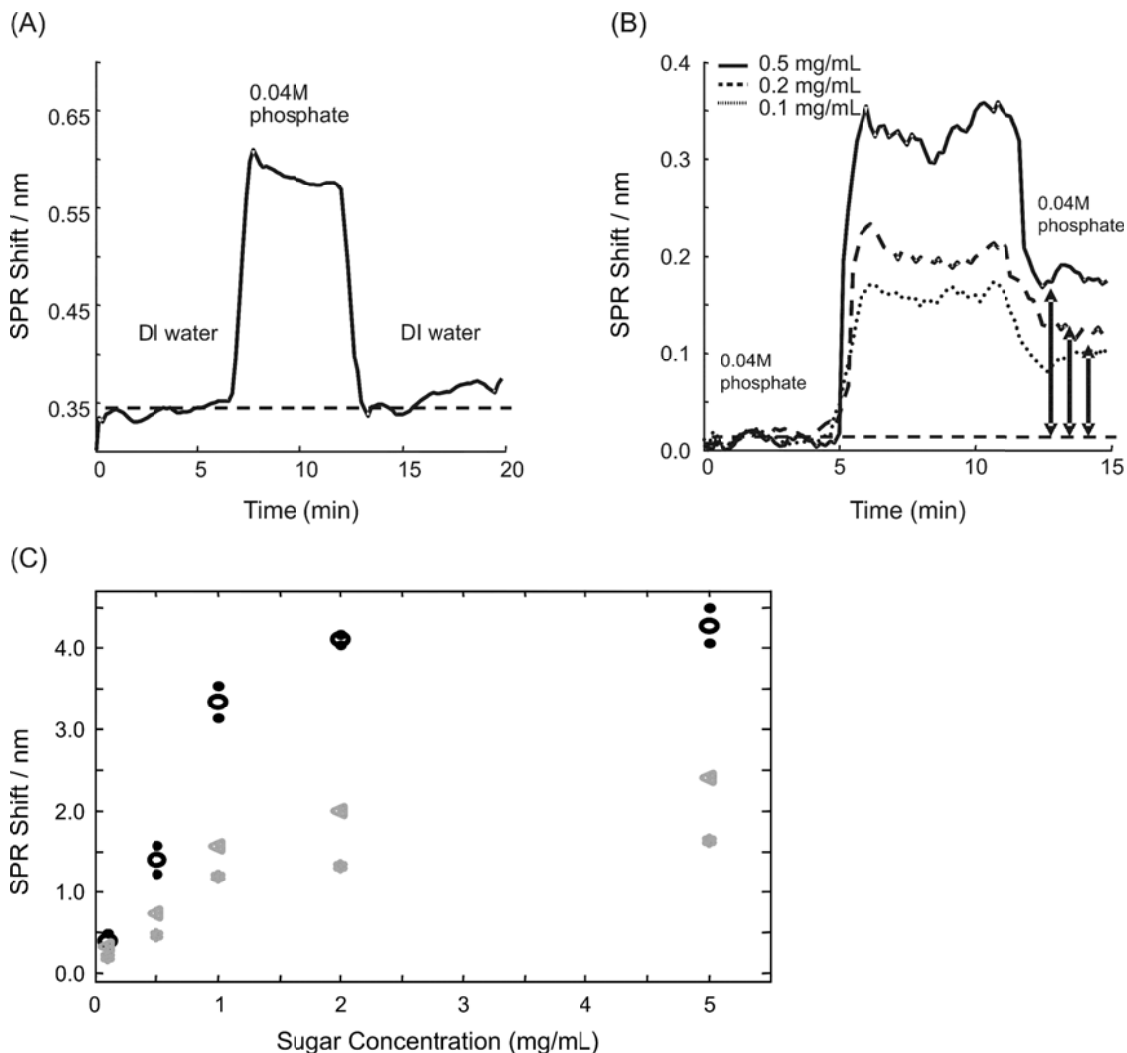
Figure 3.4. Sensor performances in presence of interferences. (A) SPR response of MIH sensor to 60 mM aqueous phosphate only. (B) SPR response of MIH sensor to glucose added to 40mM aqueous phosphate solution in different concentrations (0.1, 0.2 and 0.5 mg/ml). (C) SPR response of Au-MIH sensor to glucose (black circles), fructose (grey triangles) and sucrose (grey stars). Results were obtained from different MIH coatings. Precision of SPR shift is shown by plus/minus standard deviation of the mean (black dots, usually n=3 for glucose samples). Individual sucrose and fructose samples were not replicated.

In addition to phosphate, urine also contains a number of molecular species with amine groups (urea, uric acid and creatinine). To test their effect on the MIH coatings, a mixture of these compounds at concentrations commonly found in urine [55] was prepared and presented to the sensor similarly to the phosphate experiments described above (except for replacing titrated phosphate solution with the mixture), and it was indicated by the results that these compounds showed no net affect either.

Finally, glucose detection in human urine was explored. Figure 3.5 shows the response of MIH-coatings without and with gold nanoparticle to urine spiked with glucose. The measured response to the presence of glucose decreases significantly compared to sample solutions prepared with deionized water. The limit of detection and limit of quantification for urine analysis with the Au-MIH were determined to be 0.12 mg/mL and 0.40 mg/mL, respectively, with a sensitivity of approximately 0.34 nm/(mg/mL glucose). There are three possible contributing factors, all acting to decrease the MIH sensitivity to glucose. PAA hydrogels undergo contraction when exposed to salt solutions due to increased osmotic pressure [77]. Therefore, it is possible that MIH coatings in urine are prevented from swelling when incorporating glucose to the same extent as in deionized water. Similarly, it is likely that some of the binding cavities distort, and possibly, collapse rending them incapable of interacting with the analyte. Additionally, to the extent that hydrogen bonding between glucose and the amine functional groups in the MIH influence sensitivity, increasing ionic strength decreases the amount of intermolecular hydrogen bonding [78].
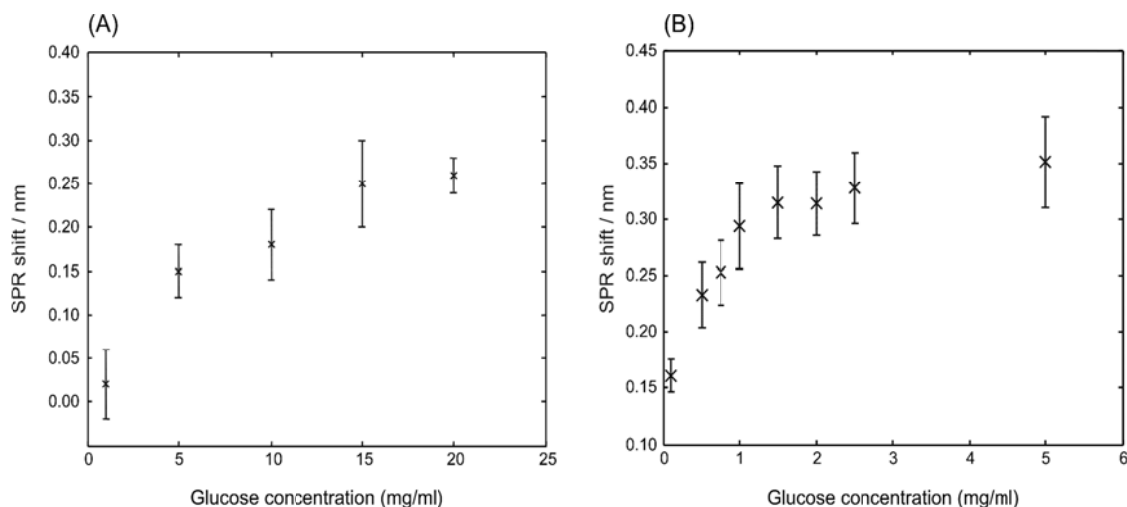
Figure 3.5. Response of (A) MIH and (B) Au-MIH coated glucose sensor in undiluted urine spiked with different concentration of glucose.

The limit of detection for the Au-MIH membranes (0.12 mg/mL) is within levels anticipated for glucose content in the urine of healthy individuals (0.06 mg/mL to 0.15 mg/mL [79,75,80,81]) and is comparable to other recent reports [82-86]. The decreased dynamic range, however, renders quantification of glucose at elevated levels difficult. Considering that glucose levels can spike to over 6 mg/mL [82] shortly after ingesting a meal and the sensor's inability to differentiate between glucose concentrations above ~1 mg/mL, indicate that in its current iteration the sensor would only reliably function for threshold-type measurements. That is, the sensor is capable of discriminating between glucose levels in healthy or diabetic individuals, but is currently unsuitable for precise monitoring.

A potential route towards further refining the sensor response involves focusing of the plasmonic wave in the gap between the underlying metal film and the embedded nanoparticles, thereby accessing the gap-mode [72]. In this arrangement, the plasmon

coupling conditions are intimately related to the distance between the two plasmon-supporting structures [72,87,88]. By using MIHs as the spacer between the two structures, it may be possible to record minor swelling due to glucose binding with high sensitivity. However, since significant enhancement of the electric field is observed primarily if the metallic film and nanoparticles are placed in close proximity (herein d ~13 nm [72]) the limited thickness of the MIH coating, and therefore, the limited number of binding sites, may ultimately negate any benefit obtained from the enhanced optical sensitivity.

Alternatively, the optical properties of gold reveal that SPR spectroscopy performed with near-infrared wavelengths displays an increased sensitivity towards RI changes compared excitation of surface plasmons in the visible range [89,90]. In addition, the d_p of the plasmonic wave in the near-infrared extends further (e.g. d_p = 1600 nm at λ_{SPR} = 1560 nm for water) into the surrounding dielectric. Since a greater portion of the MIH coating can be probed with higher sensitivity, the span of analyte concentrations that can be monitored may also be extended, ultimately improving the performance of the sensor to more closely match the requirements for glucose monitoring in urine.

Chapter 4

CONCLUSION

A SPR sensing system with hydrophilic molecularly imprinted hydrogel as recognition unit was developed for glucose monitoring. Swelling of the hydrogel sensing layer due to combination with glucose was tracked by SPR spectroscopy. While further refinements are necessary to improve sensitivity of the chemical recognition layer, the system displays potential as a specific detection method for glucose monitoring in a complex physiological fluid. Cooperation of gold nanoparticles has significantly enhanced the sensor's response and sensitivity at low glucose concentrations. The sensor showed selective response to glucose compared to fructose and sucrose, and was capable to detect glucose spiked in deionized water at the μg/mL level. Initial analysis of glucose in urine indicates that high ionic strength media disrupts the re-binding event, decreasing the MIH sensitivity. However, despite a reduced analytical performance, the Au-MIH membranes developed display comparable results to other sensing schemes aimed at analysis of glucose in urine.

REFERENCES

1.   Giraudi, G., et al., *A general method to perform a noncompetitive immunoassay for small molecules.* Analytical Chemistry, 1999. **71**(20): p. 4697-4700.

2.   Altria, K.D. and D. Elder, *Overview of the status and applications of capillary electrophoresis to the analysis of small molecules.* Journal of Chromatography A, 2004. **1023**(1): p. 1-14.

3.   Su, A.K., J.T. Liu, and C.H. Lin, *Rapid drug-screening of clandestine tablets by MALDI-TOF mass spectrometry.* Talanta, 2005. **67**(4): p. 718-724.

4.   Baker, B.R., et al., *An electronic, aptamer-based small-molecule sensor for the rapid, label-free detection of cocaine in adulterated samples and biological fluids.* Journal of the American Chemical Society, 2006. **128**(10): p. 3138-3139.

5.   Grant, D.C. and R.J. Helleur, *Simultaneous analysis of vitamins and caffeine in energy drinks by surfactant-mediated matrix-assisted laser desorption/ionization.* Analytical and Bioanalytical Chemistry, 2008. **391**(8): p. 2811-2818.

6.   Fintschenko, Y., A.J. Krynitsky, and J.W. Wong, *Emerging Pesticide Residue Issues and Analytical Approaches.* Journal of Agricultural and Food Chemistry, 2010. **58**(10): p. 5859-5861.

7.   Vonaparti, A., et al., *Preventive doping control screening analysis of prohibited substances in human urine using rapid-resolution liquid chromatography/high-resolution time-of-flight mass spectrometry.* Rapid Communications in Mass Spectrometry, 2010. **24**(11): p. 1595-1609.

8.   Banerji, S., et al., *Evaluation of polymer coatings for ammonia vapor sensing with surface plasmon resonance spectroscopy.* Sensors and Actuators B-Chemical, 2010. **147**(1): p. 255-262.

9.   Choi, S.W., et al., *Detection of Mycoestrogen Zearalenone by a Molecularly Imprinted Polypyrrole-Based Surface Plasmon Resonance (SPR) Sensor.* Journal of Agricultural and Food Chemistry, 2009. **57**(4): p. 1113-1118.

10. Hsieh, H.V., et al., *Direct detection of glucose by surface plasmon resonance with bacterial glucose/galactose-binding protein.* Biosensors & Bioelectronics, 2004. **19**(7): p. 653-660.

11. Mauriz, E., et al., *Determination of carbaryl in natural water samples by a surface plasmon resonance flow-through immunosensor.* Biosensors & Bioelectronics, 2006. **21**(11): p. 2129-2136.

12. Mauriz, E., et al., *Real-time detection of chlorpyrifos at part per trillion levels in ground, surface and drinking water samples by a portable surface plasmon resonance immunosensor.* Analytica Chimica Acta, 2006. **561**(1-2): p. 40-47.

13. Mauriz, E., et al., *Single and multi-analyte surface plasmon resonance assays for simultaneous detection of cholinesterase inhibiting pesticides.* Sensors and Actuators B-Chemical, 2006. **118**(1-2): p. 399-407.

14. Schasfoort, R.B.M. and A.J. Tudos, *Handbook of Surface Plasmon Resonance*, ed. R.B.M. Schasfoort and A.J. Tudos. 2008, Cambridge: Royal Society of Chemistry. 403.

15. Homola, J., *Surface plasmon resonance sensors for detection of chemical and biological species.* Chemical Reviews, 2008. **108**(2): p. 462-493.

16. Green, R.J., et al., *Surface plasmon resonance analysis of dynamic biological interactions with biomaterials.* Biomaterials, 2000. **21**(18): p. 1823-1835.

17. Masson, J.F., et al., *Quantitative measurement of cardiac markers in undiluted serum.* Analytical Chemistry, 2007. **79**(2): p. 612-619.

18. Fan, X.D., et al., *Sensitive optical biosensors for unlabeled targets: A review.* Analytica Chimica Acta, 2008. **620**(1-2): p. 8-26.

19. Mitchell, J., *Small Molecule Immunosensing Using Surface Plasmon Resonance.* Sensors, 2010. **10**(8): p. 7323-7346.

20. Homola, J., *Surface Plasmon Resonance Based Sensors.* Chemical Sensors and Biosensors, ed. O.S. Wolfbeis. Vol. 4. 2006, Berlin: Springer. 251.

21. Gupta, R. and A. Kumar, *Molecular imprinting in sol-gel matrix.* Biotechnology Advances, 2008. **26**(6): p. 533-547.

22. Shoji, R., T. Takeuchi, and I. Kubo, *Atrazine sensor based on molecularly imprinted polymer-modified gold electrode.* Analytical Chemistry, 2003. **75**(18): p. 4882-4886.

23. Sode, K., et al., *Construction of a molecular imprinting catalyst using target*

analogue template and its application for an amperometric fructosylamine sensor. Biosensors & Bioelectronics, 2003. **18**(12): p. 1485-1490.

24.   Ersoz, A., et al., *Molecularly imprinted ligand-exchange recognition assay of glucose by quartz crystal microbalance.* Biosensors & Bioelectronics, 2005. **20**(11): p. 2197-2202.

25.   Javanbakht, M., et al., *Molecularly imprinted polymer based potentiometric sensor for the determination of hydroxyzine in tablets and biological fluids.* Analytica Chimica Acta, 2008. **612**(1): p. 65-74.

26.   Kugimiya, A. and T. Takeuchi, *Surface plasmon resonance sensor using molecularly imprinted polymer for detection of sialic acid.* Biosensors & Bioelectronics, 2001. **16**(9-12): p. 1059-1062.

27.   Raitman, O.A., et al., *Analysis of NAD(P)(+) and NAD(P)H cofactors by means of imprinted polymers associated with Au surfaces: A surface plasmon resonance study.* Analytica Chimica Acta, 2004. **504**(1): p. 101-111.

28.   Pernites, R.B., R.R. Ponnapati, and R.C. Advincula, *Surface plasmon resonance (SPR) detection of theophylline via electropolymerized molecularly imprinted polythiophenes.* Macromolecules, 2010. **43**(23): p. 9724-9735.

29.   Heller, A. and B. Feldman, *Electrochemical Glucose Sensors and Their Applications in Diabetes Management.* Chemical Reviews, 2008. **108**(7): p. 2482-2505.

30.   Oliver, N.S., et al., *Glucose sensors: a review of current and emerging technology.* Diabetic Med., 2009. **26**(3): p. 197-210.

31.   Toghill, K.E. and R.G. Compton, *Electrochemical Non-enzymatic Glucose Sensors: A Perspective and an Evaluation.* International Journal of Electrochemical Science, 2010. **5**(9): p. 1246-1301.

32.   Yoshimi, Y., et al., *Development of an enzyme-free glucose sensor using the gate effect of a molecularly imprinted polymer.* Journal of Artificial Organs, 2009. **12**(4): p. 264-270.

33.   Rathod, D., et al., *Platinum nanoparticle decoration of carbon materials with applications in non-enzymatic glucose sensing.* Sensors and Actuators B-Chemical, 2010. **143**(2): p. 547-554.

34.   Feng, D., F. Wang, and Z.L. Chen, *Electrochemical glucose sensor based on one-step construction of gold nanoparticle-chitosan composite film.* Sensors and Actuators B-Chemical, 2009. **138**(2): p. 539-544.

35. Hoffman, A.S., *Hydrogels for biomedical applications.* Advanced Drug Delivery Reviews, 2002. **54**(1): p. 3-12.

36. Gerlach, G., K.-F. Arndt, and Editors, *Hydrogel Sensors And Actuators.* Springer Series on Chemical Sensors and Biosensors, ed. G. Urban. Vol. 6. 2009, Berlin: Springer-Verlag. 272.

37. Molinelli, A., et al., *Analyzing the Mechanisms of Selectivity in Biomimetic Self-Assemblies via IR and NMR Spectroscopy of Prepolymerization Solutions and Molecular Dynamics Simulations.* Analytical Chemistry, 2005. **77**(16): p. 5196-5204.

38. O'Mahony, J., et al., *Towards the rational development of molecularly imprinted polymers: 1H NMR studies on hydrophobicity and ion-pair interactions as driving forces for selectivity.* Biosensors & Bioelectronics, 2005. **20**(9): p. 1884-1893.

39. O'Mahony, J., et al., *Anatomy of a successful imprint: Analysing the recognition mechanisms of a molecularly imprinted polymer for quercetin.* Biosensors & Bioelectronics, 2006. **21**(7): p. 1383-1392.

40. Wang, J. and H.S. Zhou, *Aptamer-Based Au Nanoparticles-Enhanced Surface Plasmon Resonance Detection of Small Molecules.* Analytical Chemistry, 2008. **80**(18): p. 7174-7178.

41. Mitchell, J., *Small molecule immunosensing using surface plasmon resonance.* Sensors, 2010. **10**: p. 7323-7346.

42. Baba, A., et al., *Electrochemical Surface Plasmon Resonance and Waveguide-Enhanced Glucose Biosensing with N-Alkylaminated Polypyrrole/Glucose Oxidase Multilayers.* ACS Applied Materials & Interfaces, 2010. **2**(8): p. 2347-2354.

43. Banerji, S., et al., *Evaluation of polymer coatings for ammonia vapor sensing with surface plasmon resonance spectroscopy.* Sensors and Actuators, B: Chemical, 2010. **B147**(1): p. 255-262.

44. Matsui, J., et al., *Molecularly imprinted nanocomposites for highly sensitive SPR detection of a non-aqueous atrazine sample.* Analyst, 2009. **134**(1): p. 80-86.

45. Lyon, L.A., M.D. Musick, and M.J. Natan, *Colloidal Au-enhanced surface plasmon resonance immunosensing.* Analytical Chemistry, 1998. **70**(24): p. 5177-5183.

46. Lyon, L.A., W.D. Holliway, and M.J. Natan, *An improved surface plasmon*

resonance imaging apparatus. Review of Scientific Instruments, 1999. **70**(4): p. 2076-2081.

47.   Tokareva, I., et al., *Ultrathin molecularly imprinted polymer sensors employing enhanced transmission surface plasmon resonance spectroscopy.* Chemical Communications, 2006(31): p. 3343-3345.

48.   Matsui, J., et al., *Composite of Au nanoparticles and molecularly imprinted polymer as a sensing material.* Analytical Chemistry, 2004. **76**(5): p. 1310-1315.

49.   Chah, S., et al., *The effect of substrate metal on 2-aminoethanethiol and nanoparticle enhanced surface plasmon resonance imaging.* Chemical Physics, 2001. **272**(1): p. 127-136.

50.   Matsui, J., et al., *SPR sensor chip for detection of small molecules using molecularly imprinted polymer with embedded gold nanoparticles.* Analytical Chemistry, 2005. **77**(13): p. 4282-4285.

51.   Battaglia, T.M., et al., *Quantification of cytokines involved in wound healing using surface plasmon resonance.* Analytical Chemistry, 2005. **77**(21): p. 7016-7023.

52.   Parmpi, P. and P. Kofinas, *Biomimetic glucose recognition using molecularly imprinted polymer hydrogels.* Biomaterials, 2004. **25**(10): p. 1969-1973.

53.   Feas, X., et al., *Molecularly imprinted polyallylamine hydrogels: another reassessment.* Polymer International, 2010. **59**(1): p. 11-15.

54.   Ji, X.H., et al., *Size control of gold nanocrystals in citrate reduction: The third role of citrate.* Journal of the American Chemical Society, 2007. **129**(45): p. 13939-13948.

55.   Putnam, D.F., *Composition and concentrative properties of human urine.* 1971, Adv. Biotechnol. Power Dep., McDonnell Douglas Astronaut. Co., Huntington Beach, CA, USA. p. 107 pp.

56.   Lin-Vien, D., *The Handbook of infrared and raman characteristic frequencies of organic molecules.* 1991, Boston: Academic Press.

57.   Iio, K., N. Minoura, and M. Nagura, *SWELLING CHARACTERISTICS OF A BLEND HYDROGEL MADE OF POLY(ALLYLBIGUANIDO-CO-ALLYLAMINE) AND POLY(VINYL ALCOHOL).* Polymer, 1995. **36**(13): p. 2579-2583.

58.   Kobayashi, S., et al., *POLY(ALLYLAMINE) - CHELATING PROPERTIES*

AND RESINS FOR URANIUM RECOVERY FROM SEAWATER. Macromolecules, 1985. **18**(12): p. 2357-2361.

59. Aleman, C., J.J. Navas, and S. Munozguerra, *Study of the Amide...Ester Hydrogen Bond in Small Molecules and Its Influence on the Conformation of Polypeptides and Related Polymers.* Journal of Physical Chemistry, 1995. **99**(49): p. 17653-17661.

60. Aleman, C., et al., *Toward an understanding of the drug-DNA recognition mechanism. Hydrogen-bond strength in netropsin-DNA complexes.* Journal of Physical Chemistry, 1996. **100**(27): p. 11480-11487.

61. He, L., et al., *Colloidal Au-enhanced surface plasmon resonance for ultrasensitive detection of DNA hybridization.* Journal of the American Chemical Society, 2000. **122**(38): p. 9071-9077.

62. Zinman, B., et al., *American Diabetes Association. Standards of medical care in diabetes-2010 (vol 33, pg S11, 2010).* Diabetes Care, 2010. **33**(3): p. 692-692.

63. Kuzuya, T., et al., *Report of the Committee on the classification and diagnostic criteria of diabetes mellitus.* Diabetes Research and Clinical Practice, 2002. **55**(1): p. 65-85.

64. Urakami, T., et al., *Annual incidence and clinical characteristics of type 2 diabetes in children as detected by urine glucose screening in the Tokyo metropolitan area.* Diabetes Care, 2005. **28**(8): p. 1876-1881.

65. Davidson, J.K., *Clinical diabetes mellitus : a problem-oriented approach.* 2000, New York: Thieme.

66. Xiao, F., et al., *Nonenzymatic glucose sensor based on ultrasonic-electrode position of bimetallic PtM (M = Ru, Pd and Au) nanoparticles on carbon nanotubes-ionic liquid composite film.* Biosensors & Bioelectronics, 2009. **24**(12): p. 3481-3486.

67. Cheng, Z.L., E.K. Wang, and X.R. Yang, *Capacitive detection of glucose using molecularly imprinted polymers.* Biosensors & Bioelectronics, 2001. **16**(3): p. 179-185.

68. Shoji, E. and M.S. Freund, *Potentiometric saccharide detection based on the pKa changes of poly(aniline boronic acid).* Journal of the American Chemical Society, 2002. **124**(42): p. 12486-12493.

69. Li, Y., et al., *Hydrogen bubble dynamic template synthesis of porous gold for nonenzymatic electrochemical detection of glucose.* Electrochemistry

Communications, 2007. **9**(5): p. 981-988.

70. Wolfbeis, O.S., M. Schaferling, and A. Durkop, *Reversible optical sensor membrane for hydrogen peroxide using an immobilized fluorescent probe, and its application to a glucose biosensor.* Microchimica Acta, 2003. **143**(4): p. 221-227.

71. Hill, R.T., et al., *Leveraging Nanoscale Plasmonic Modes to Achieve Reproducible Enhancement of Light.* Nano Letters, 2010. **10**(10): p. 4150-4154.

72. Kawata, S.E., *Near-Field Optics and Surface Plasmon Polaritons.* Topics in Applied Physics, ed. C.E. Ascheron and H.J. Koelsch. Vol. 81. 2001, Berlin: Springer-Verlag 210.

73. Yan, M. and R. Olof, eds. *Molecularly Imprinted Materials: Science and Technology.* 2005, CRC Press: New York. 752.

74. Sellergren, B., ed. *Molecularly Imprinted Polymers: Man-Made Mimics of Antibodies and Their Applications in Analytical Chemistry.* Techniques and Instrumentation in Analytical Chemistry. Vol. 23. 2001, Elsevier Science: Amsterdam. 582.

75. Manju, S., P.R. Hari, and K. Sreenivasan, *Fluorescent molecularly imprinted polymer film binds glucose with a concomitant changes in fluorescence.* Biosensors & Bioelectronics, 2010. **26**(2): p. 894-897.

76. Shimizu, K.D. and C.J. Stephenson, *Molecularly imprinted polymer sensor arrays.* Current Opinion in Chemical Biology, 2010. **14**(6): p. 743-750.

77. Rao, G.V.R., T. Konishi, and N. Ise, *Ordering in Poly(allylamine hydrochloride) Gels.* Macromolecules, 1999. **32**(22): p. 7582-7586.

78. Qun, G. and W. Ajun, *Effects of molecular weight, degree of acetylation and ionic strength on surface tension of chitosan in dilute solution.* Carbohydrate Polymers, 2006. **64**(1): p. 29-36.

79. Moreno-Bondi, M.C., et al., *Oxygen optrode for use in a fiber-optic glucose biosensor.* Analytical Chemistry, 1990. **62**(21): p. 2377-80.

80. Fine, J., *Glucose content of normal urine.* British Medical Journal, 1965. **1965-1**(5444): p. 1209-14.

81. Sen, D.K. and G.S. Sarin, *Tear glucose levels in normal people and in diabetic patients.* The British journal of ophthalmology, 1980. **64**(9): p. 693-5.

82. Miyashita, M., et al., *Development of urine glucose meter based on micro-planer amperometric biosensor and its clinical application for self-monitoring of urine glucose.* Biosensors & Bioelectronics, 2009. **24**(5): p. 1336-1340.

83. Xiao, F., et al., *Nonenzymatic glucose sensor based on ultrasonic-electrodeposition of bimetallic PtM (M=Ru, Pd and Au) nanoparticles on carbon nanotubes-ionic liquid composite film.* Biosensors & Bioelectronics, 2009. **24**(12): p. 3481-3486.

84. Irawan, R., et al., *Polymer waveguide sensor for early diagnostic and wellness monitoring.* Biosensors & Bioelectronics, 2011. **26**: p. 3666-3669.

85. Liu, Y., et al., *Specific Detection of D-Glucose by a Tetraphenylethene-Based Fluorescent Sensor.* Journal of the American Chemical Society, 2011. **133**(4): p. 660-663.

86. Gao, X., et al., *A wireless magnetoelastic biosensor for rapid detection of glucose concentrations in urine samples.* Sensors and Actuators, B: Chemical, 2007. **B128**(1): p. 161-167.

87. Holland, W.R. and D.G. Hall, *Frequency shifts of an electric-dipole resonance near a conducting surface.* Physical Review Letters, 1984. **52**(12): p. 1041-4.

88. Holland, W.R. and D.G. Hall, *Surface-plasmon dispersion relation: Shifts induced by the interaction with localized plasma resonances.* Physical Review B: Condensed Matter and Materials Physics, 1983. **27**(12): p. 7765-8.

89. Nelson, B.P., et al., *Near-Infrared Surface Plasmon Resonance Measurements of Ultrathin Films. 1. Angle Shift and SPR Imaging Experiments.* Analytical Chemistry, 1999. **71**(18): p. 3928-3934.

90. Menegazzo, N., et al., *Characterization of a Variable Angle Reflectance Fourier Transform Infrared Accessory Modified for Surface Plasmon Resonance Spectroscopy.* Applied Spectroscopy, 2010. **64**(10): p. 1181.